Inorg. Chem. **2005**, *44*, 2926–2933

The Insertion of Carbodiimides into Al and Ga Amido Linkages. Guanidinates and Mixed Amido Guanidinates of Aluminum and Gallium

Amanda P. Kenney,[†] Glenn P. A. Yap,[‡] Darrin S. Richeson,[‡] and Seán T. Barry*,[†]

Department of Chemistry, Carleton University, Ottawa, Ontario K1S 5B6, Canada, and Department of Chemistry, University of Ottawa, Ottawa, Ontario K1N 6N5, Canada

Received November 8, 2004

The insertion of carbodiimides into existing metal–heteroatom bonds is an important preparative route for the synthesis of useful ligand systems such as amidinates and guanidinates. Our interest lies in multiple insertions at one metal center and the mechanisms of insertion and rearrangement. We have synthesized and characterized $[Me_2NC(N^iPr)_2]_nM(NMe_2)_{3-n}$ (n = 1, 2, 3; M = Al, Ga). We have investigated the mechanism of synthesis and discovered a ligand transfer step that is important for the formation of the final products.

Introduction

Group 13 amidinate and guanidinate complexes are novel catalysts and potential gaseous precursors to technologically important materials.[1,2] In particular, these compounds can act as precursors to group 13 nitrides, which are direct band gap semiconductors, as well as precursors to thin metal films, in the case of aluminum precursors. Mixed aluminum/gallium nitrides have been applied as tunable band gap materials in high-frequency LEDs and diode lasers.[3]

Monoanionic, N-substituted guanidinate anions $[RNC(NR'_2)NR]^-$ should be useful ligands for designing monomeric, volatile precursors of group 13 metals. These nitrogen-rich species are three-atom, chelating ligands that can be subjected to rational substituent modifications in order to control the steric and electronic properties of their metal complexes and, ultimately, the physical properties of these species.[4] The bidentate nature of these ligands should favor an electronically saturated metal coordination sphere, which will encourage mononuclear, low molecular weight species. Furthermore, these species and their complexes are relatively simple to synthesize, should exhibit increased stability, and, with a judicious choice of substituents, should be amenable to the design of precursors with reproducible gas-phase concentrations.

Guanidinate complexes can be prepared by the insertion of carbodiimides into main-group metal amido linkages,[5] and there is one previous report for the synthesis of an aluminum guanidinate via the insertion of carbodiimides into an existing Al−N bond.[6] Although previously ignored, the reversibility of this insertion mechanism is of interest as a potential thermal decomposition route. Such a deinsertion reaction provides an accessible transformation pathway for chemical vapor deposition source molecules that possess guanidinate ligands, offering an added attraction to these precursor species. In addition, multiple insertions of carbodiimides at a single metal center to form bis- and tris(guanidinato) species of aluminum and gallium could lead to more stable, coordinatively saturated compounds.

The synthetic mechanism and thermal reactivity require more scrutiny in this family of compounds, and so we report the synthesis and structural characterization of novel mixed amido−guanidinato compounds of aluminum and gallium, $[Me_2NC(N^iPr)_2]_nM(NMe_2)_{3-n}$ (n = 1, 2, 3), prepared via the insertion of diisopropylcarbodiimide into the metal amido bonds of $M_2(NMe_2)_6$ (M = Al, Ga). Additionally, thermolysis of these compounds in sealed NMR tubes will be discussed.

* Author to whom correspondence should be addressed. Fax: (613)-520-2569. Email: sbarry@ccs.carleton.ca.

† Carleton University.

‡ University of Ottawa.

(1) (a) Aeilts, S. L.; Coles, M. P.; Swenson, D. C.; Jordan, R. F. *Organometallics* **1998**, *17*, 3265. (b) Coles, M. P.; Jordan, R. F. *J. Am. Chem. Soc.* **1997,** *119*, 8125. (c) Dagorne, S.; Guzei, I. A.; Coles, M. P.; Jordan, R. F. *J. Am. Chem. Soc.* **2000**, *122*, 274.

(2) (a) Meier, R. J.; Koglin, E. *J. Phys. Chem. A* **2001**, *105*, 3867. (b) Barker, J.; Blacker, N. C.; Phillips, P. R.; Alcock, N. W.; Errington, W.; Wallbridge, M. G. H. *J. Chem. Soc., Dalton Trans.* **1996**, 431.

(3) Nakamura, S.; Senoh, M.; Nagahama, S.; Iwasa, N.; Yamada, T.; Matsushita, T.; Sugimoto, Y.; Kiyoku, H. *Appl. Phys. Lett.* **1996**, *69*, 4056.

(4) For a recent review of guanidinate complexes, see: Bailey, P. J.; Pace, S. *Coord. Chem. Rev.* **2001**, *214*, 91 and references therein.

(5) For examples of the insertion of carbodiimides into M−N bonds with M = Si, Ge, Sn, see: (a) Matsuda, I.; Itoh, K.; Ishii, Y. *J. Organomet. Chem.* **1974**, *69*, 353. (b) Chandra, G.; Jenkins, A. D.; Lappert, M. F.; Srivastava, R. C. *J. Chem. Soc. A* **1970**, 2550. (c) George, T. A.; Jones, K.; Lappert, M. F. *J. Chem. Soc.* **1965**, 2157.

(6) (a) Chang, C. C.; Hsiung, C. S.; Su, H. L.; Srinivas, B.; Chiang, M. Y.; Lee, G. H.; Wang, Y. *Organometallics* **1998**, *17*, 1595. (b) Chang, C. C.; Ameerunisha, M. S. *Coord, Chem. Rev.* **1999**, *189*, 199.

10.1021/ic048433g CCC: $30.25
Published on Web 03/22/2005

Scheme 1. Stoichiometric Control of Carbodiimide Insertion into Metal−Amide Bonds

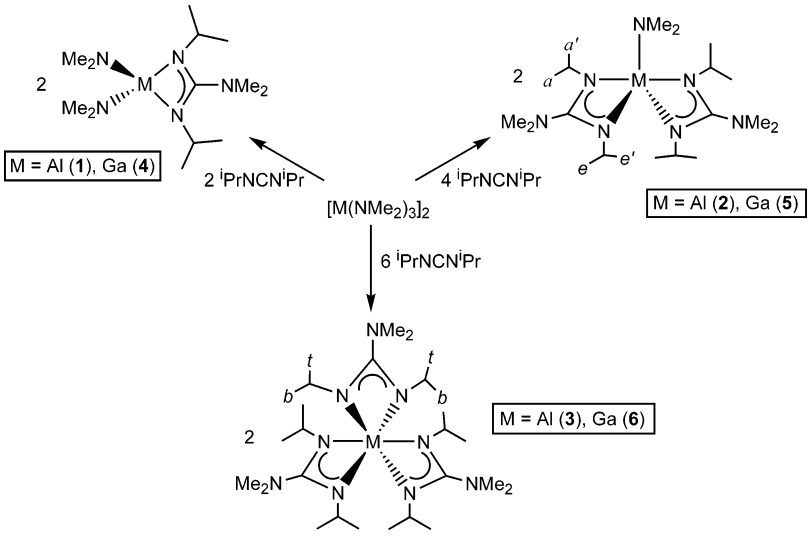

Results and Discussion

We have determined that the homoleptic amido dimers $M_2(NMe_2)_6$ (M = Al, Ga) react readily with two, four, and six equiv of diisopropylcarbodiimide to yield six new guanidinato complexes of these group 13 metals, as illustrated in Scheme 1. Compounds **1**−**6** have been isolated in good to excellent yields as clear and colorless crystalline materials with relatively low melting points for the mono- and bis(guanidinato) species (45−70 °C) and somewhat higher values (137 and 193 °C) for the tris(guanidinato) compounds. Each of these compounds exhibited distinctive ^{1}H and ^{13}C NMR signatures that are consistent with the suggested formulations. In addition, the similarities between these spectra indicate that the related Al and Ga compounds have analogous solution structures. Furthermore, all six complexes have been characterized by single-crystal X-ray diffraction analysis, and these results are presented below.

As anticipated for a monomeric, distorted tetrahedral metal environment of C_{2v} symmetry, the NMR spectra of compounds **1** and **4** indicate a single environment for the ^{i}Pr substituents of the guanidinato ligand. The NMR spectra of **2** and **5** suggested that they have fluxional solution structures. In particular, the static distorted trigonal bipyramidal structures of these two compounds should yield two spectroscopically distinguished ^{i}Pr substituents with four diastereotopic Me groups corresponding to *a*, *a*′, *e*, and *e*′, as indicated in Scheme 1. The experimental observation of a single set of isopropyl resonances including only one doublet for the methyl groups indicates a fluxional process that equilibrates axial/equatorial sites as well as the two faces of the guanidinato ligand.[7]

The ^{1}H NMR spectra of the six coordinate, tris(chelate) complexes **3** and **6** support the structure shown in Scheme 1 and, in the case of compound **6**, display features consistent with a dynamic solution structure. The spectra for these species display one equivalent environment for the three guanidinato ligands, and the appearance of one singlet for the dimethylamino group is consistent with the free rotation of the C−NMe_2 bond at room temperature. Furthermore, the ^{i}Pr groups of **3** display a single septet for the CH moiety with two well-resolved doublets at 1.46 and 1.37 ppm having equal intensity for the methyl groups. This is entirely consistent with the limiting structure illustrated in Scheme 1 in which the two inequivalent Me groups are indicated as *t* and *b*. A dynamic process that exchanges these diastereotopic methyl groups is evident in the spectra of **6** in which two broad resonances appear at 1.36 and 1.44 ppm in the room temperature ^{1}H NMR spectrum. Variable-temperature ^{1}H NMR spectra further support the fluxional behavior by demonstrating the limiting structures. As seen in Figure 1, when a sample of **6** is cooled below 280 K, the static limit is reached and the isopropyl moieties now appear as two doublets for two inequivalent Me groups. Above 320 K, an exchange process that equilibrates the two ligand faces becomes dominant and renders the Me groups equivalent. These observations are reversible. We attribute the lower barrier to rotation that is seen for **6** compared to **3** to be a result of the larger metal center and longer M−N bonds, which decrease the steric interaction with the isopropyl group.

A closer examination of the reactions illustrated in Scheme 1 revealed an unexpected pathway that interconnects the mono-, bis-, and tris(guanidinato) species. During the preparations of these species, it was noted that the reaction of the starting amido compounds with six equiv of diisopropylcarbodiimide to form the tris(guanidinato) complexes occurred very rapidly, in a matter of minutes. In contrast, reactions between the amido dimers and two equiv of carbodiimide required much longer reaction times in order to isolate good yields of compounds **1** and **4**. An examination of the NMR spectra of the 1:2 reaction mixtures at early reaction times indicated a complex reaction mixture that contained small amounts of the targeted mono(guanidinato) compounds $[(^iPrN)_2CNMe_2]M(NMe_2)_2$ as well as significant amounts of the bis- and tris(guanidinato) compounds

(7) (a) Mullins, S. M.; Duncan, A. P.; Bergman, R. G.; Arnold, J. *Inorg. Chem.* **2001**, *40*, 6952. (b) Bazinet, P.; Wood, D.; Yap, G. P. A.; Richeson, D. S. *Inorg. Chem.* **2003**, *42*, 6225.

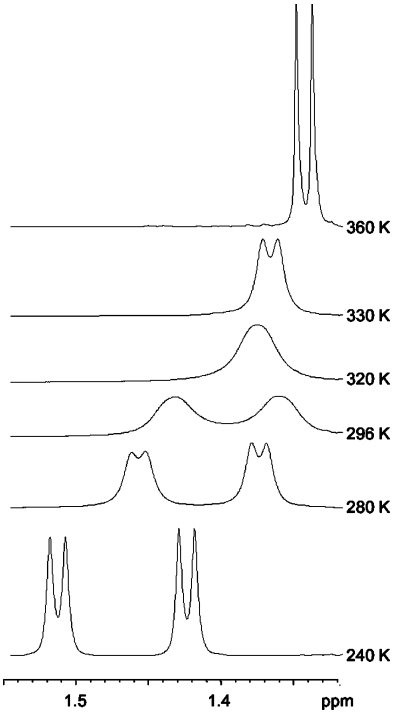

Figure 1. Variable temperature ^{1}H NMR study of compound **6**, focusing on the spectral region for the methyl signals for the isopropyl groups of the guanidinato ligands.

$[(^i\text{PrN})_2\text{CNMe}_2]_2\text{MNMe}_2$ and $[(^i\text{PrN})_2\text{CNMe}_2]_3\text{M}$, respectively. These mixtures also contained an appropriate amount of unreacted homoleptic amido compound. Furthermore, the reaction with six equiv of carbodiimide and the amido starting materials in a time scale of minutes gave the six-coordinate tris(guanidinato) species **3** and **6**, and NMR spectra that were taken at early stages of the reaction showed only the presence of **3** and **6** and starting amido complexes. In addition, monitoring the reaction of amido starting materials with four equiv of carbodiimide by NMR indicated the presence of the tris(guanidinato) complexes **3** and **6** along with unreacted homoleptic amido species. Compounds **1** and **2** were not observed in these reaction mixtures. Allowing these reactions to proceed overnight led, ultimately, to the formation of the expected bis(guanidinato) compounds **2** and **5**. This set of observations suggests that the insertion of diisopropylcarbodiimide with $M_2(NMe_2)_6$ proceeds rapidly to produce the triply inserted products **5** and **6** and unreacted starting materials. These products then undergo a ligand exchange reaction on a much slower time scale (over several hours) to ultimately lead to stoichiometrically controlled products. In all cases, the syntheses of **1**−**4** can be carried out in high yield, provided that sufficient time is allowed for the ligand redistribution and incorporation of starting amido complexes. We currently attribute the origin of these observations to a slow reaction of the dinuclear homoleptic amido species with carbodiimide. We propose that once this dimer is cleaved and has undergone an insertion of carbodiimide, subsequent insertions are very rapid and proceed to generate the tris(guanidinato) species. We then suggest that a slower guanidinate for amide ligand exchange process occurs that leads to the desired product.

Scheme 2 Proposed Ligand Exchange Mechanism as the Slow Step in Amido Guanidinate Formation

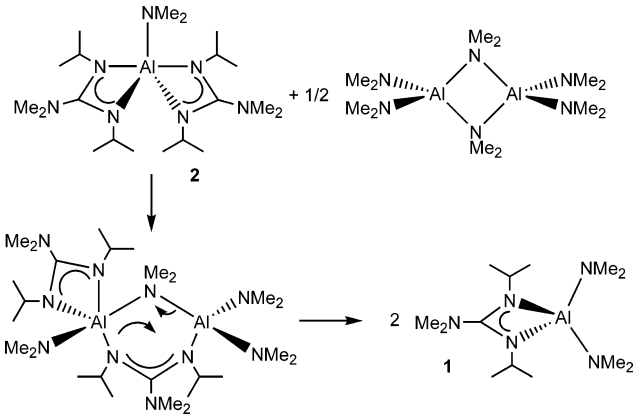

In an effort to shed some light on the process of ligand exchange, the reaction between the tris(guanidinato) complexes and the amido species, we carried out the reaction of **3** with $AlCl_3$ in stoichiometric ratios of 2:1 and 1:2. The sole isolated products in these two reactions were $[(^i\text{PrN})_2\text{CNMe}_2]_2\text{AlCl}$ (**7**) and $[(^i\text{PrN})_2\text{CNMe}_2]\text{AlCl}_2$[1a] (**8**), respectively. Jordan's group previously synthesized $[(^i\text{PrN})_2\text{CNMe}_2]\text{AlCl}_2$ using salt metathesis between the lithium guanidinate and aluminum chloride, while complex **7** is a new species that was isolated in excellent yield and which we have fully characterized spectroscopically and through single-crystal X-ray diffraction, the results of which are presented below. There was no evidence for the formation of free carbodiimide in either of these reactions, nor were there any products that possessed chloroamidinate ligands, $(^i\text{PrN})_2\text{CCl}^-$, that would have been derived from carbodiimide insertion into an Al−Cl bond.[6] Our current proposal for the guanidinate exchange process with tris(dimethylamido)-aluminum dimer is summarized in Scheme 2 for the conversion of **2** to **1**. This process involves the direct transfer of intact guanidinato and amido ligands through a doubly bridged intermediate that collapses with the exchange of the two groups.[8] Further thermal and kinetics studies to sort out the mechanism of this rearrangement are topics of study in our laboratory.

Structural Results

The single-crystal X-ray diffraction results for compounds **1** and **4** are summarized in Figure 2 and Tables 1 and 2. The structure of **4** is excluded from Figure 2 because it is isostructural with **1**. These results confirmed the monomeric nature of these compounds and demonstrated that the Al and Ga species have very similar structures, as was suggested by the NMR data. For example, both complexes have the metal center in a distorted tetrahedral environment provided by two amido ligands and a bidentate guanidinate ligand, with the restricted bite angle of the guanidinate ligand as the origin of the major deviations from ideality. In **1**, the amido nitrogen centers N4 and N5 are planar, as indicated by the sum of the angles around these atoms of 358.5° and

(8) For a recent example of bridiging guanidinates, see: Coles, M. P.; Hitchcock, P. B. *Eur. J. Inorg. Chem.* **2004**, 2662.

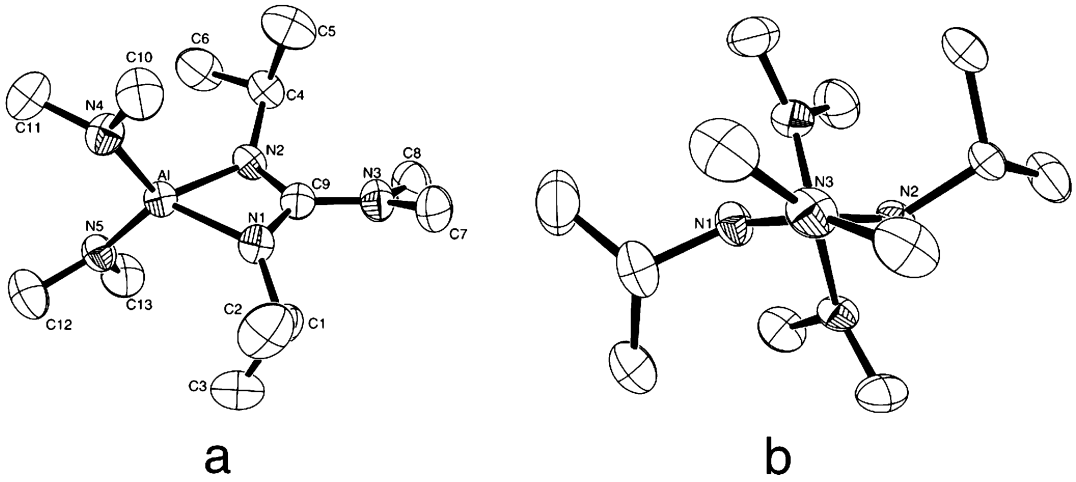

Figure 2. (a) Molecular structure and atom numbering scheme for compound **1**. (b) A view of the structure of **1** in the guanidinate plane along the Al−C9−N3 axis is provided in order to show the distortion of N1 and N2 from planarity and the angle between the NMe_2 plane and the N1−C9−N2 plane. Hydrogen atoms have been omitted in every case for clarity, and thermal ellipsoids are shown at 50% probability.

Table 1. Crystal Data and Structure Refinement for Compounds **1**−**7**

compound	**1**	**2**	**3**	**4**
empirical formula	$C_{13}H_{32}AlN_5$	$C_{20}H_{46}AlN_7$	$C_{27}H_{60}AlN_9$	$C_{13}H_{32}GaN_5$
formula weight	285.42	205.81	537.82	328.16
T (K)	203(2)	206(2)	203(2)	203(2)
λ (Å)	0.71073	0.71073	0.71073	0.71073
crystal system	monoclinic	monoclinic	cubic	monoclinic
space group	$P2_1/n$	$C2/c$	$I\bar{4}3d$	$P2_1/n$
unit cell dimensions (Å, deg)	$a = 8.729(5)$	$a = 16.510(4)$	$a = 23.5593(1)$	$a = 8.754(2)$
	$b = 15.213(7)$	$b = 8.754(2)$	$b = 23.5593(1)$	$b = 14.065(3)$
	$c = 13.902(4)$	$c = 18.025(4)$	$c = 23.5593(1)$	$c = 15.400(4)$
	$\beta = 97.25(4)°$	$\beta = 93.185(4)°$		$\beta = 101.801(4)°$
V (Å^3)	1831.4(2)	2601.2(1)	13076(1)	1856.1(8)
Z	4	8	16	4
ρ (calculated; g/cm^3)	1.035	1.051	1.093	1.174
R1, wR2[a]	0.0721, 0.1152	0.0540, 0.1164	0.0355, 0.0963	0.0537, 0.1513

compound	**5**	**6**	**7**
empirical formula	$C_{20}H_{46}GaN_7$	$C_{27}H_{60}GaN_9$	$C_{18}H_{40}AlClN_6$
formula weight	454.36	580.56	402.99
T (K)	205(2)	203(2)	207(2)
λ (Å)	0.71073	0.71073	0.71073
crystal system	monoclinic	cubic	monoclinic
space group	$P2_1/n$	$I\bar{4}3d$	$P2_1/c$
unit cell dimensions (Å; deg)	$a = 9.345(3)$	$a = 23.7146(1)$	$a = 13.796(4)$
	$b = 16.241(4)$	$b = 23.7146(1)$	$b = 9.531(3)$
	$c = 17.524(5)$	$c = 23.\ 7146(1)$	$c = 18.470(5)$
	$\beta = 5.327(6)°$		$\beta = 98.809(4)°$
V (Å^3)	2648.1(1)	13337(2)	2400.0(1)
Z	4	16	4
ρ (calculated; g/cm^3)	1.140	1.157	1.115
R1, wR2[a]	0.0568, 0.1059	0.0294, 0.0711	0.0460, 0.1068

[a] $[I > 2\sigma(I)]$. $R1 = \sum||F°| - |F_c||/\sum|F°|$. $wR2 = (\sum w(|F_o| - |F_c|)^2/\sum w|F_o|^2)^{1/2}$.

358.1°, respectively. The analogous amido centers in the Ga species (**2**) are less planar ($\sum$ angles: N4 = 356.0°; N5 = 352.9°), which is a common contrasting feature of the amido compounds of these two elements.[9]

The most remarkable feature of the structures of **1** and **4** is the deviation from planarity for the guanidinate N1 and N2 centers. Specifically, for compound **1**, the sum of angles around N1 and N2 is 351° and 346°, respectively, and the corresponding values in **4** were found to be 353° and 344°. The effect is obvious when the structure is viewed in the plane of the guanidinate ligand, and this view for complex **1** is shown in Figure 2b. It is also noteworthy that all three C−N bonds in the guanidinate ligands of **1** and **4** are equivalent with average values of 1.348(4) Å for **1** and 1.357(6) Å for **4**. The remaining bonding parameters within the guanidinate ligands in **1** and **4** are in accord with previously reported structures of guanidinate complexes.[1,4]

An understanding of the bonding parameters within the guanidinate ligands may be provided by a consideration of the potential resonance structures A−C (Scheme 3). A characteristic feature of guanidinate ligands is the presence of the NR'_2 function that is capable of donating lone pair electron density to the central carbon of the chelate ring, thus, stabilizing a zwitterionic resonance structure. This resonance structure leads to increased electron donation to the metal and leaves lone pair electron density on the two metal-bound

Table 2. Selected Bond Lengths [Å] and Angles amd Torsion Angles [deg] for Compounds **1**−**7**

$[Me_2NC(N^iPr)_2]Al(NMe_2)_2$ (**1**)		$[Me_2NC(N^iPr)_2]_2AlNMe_2$ (**2**)		$[Me_2NC(N^iPr)_2]_3Al_2$ (**3**)		$[Me_2NC(N^iPr)_2]_2AlCl$ (**7**)	
Al−N5	1.788(3)	Al−N2	1.822(2)	Al−N1	2.023(1)	Al−N3	1.979(1)
Al−N4	1.797(3)	Al−N4	2.016(2)	Al−N2	2.025(1)	Al−N4	1.927(1)
Al−N1	1.912(3)	Al−N4b	2.016(2)	N1−C9	1.329(2)	Al−N15	1.929(1)
Al−N2	1.922(3)	Al−N9	1.962(2)	N2−C9	1.332(2)	Al−N17	1.993(1)
		Al−N9b	1.962(2)	N3−C9	1.408 (2)	Al−Cl	2.206(7)

$[Me_2NC(N^iPr)_2]Ga(NMe_2)_2$ (**4**)		$[Me_2NC(N^iPr)_2]_2GaNMe_2$ (**5**)		$[Me_2NC(N^iPr)_2]_3Ga$ (**6**)	
Ga−N4	1.847(4)	Ga−N3	1.859(3)	Ga−N1	2.086(1)
Ga−N5	1.858(4)	Ga−N5	2.145(3)	Ga−N2	2.095(1)
Ga−N1	1.994(4)	Ga−N10	1.986(3)	N1−C9	1.336(2)
Ga−N2	1.996(4)	Ga−N17	1.979(3)	N2−C9	1.329(2)
Ga−N22	2.165(3)	N3−C9	1.396(2)		

$[Me_2NC(N^iPr)_2]Al(NMe_2)_2$ (**1**)		$[Me_2NC(N^iPr)_2]_2AlNMe_2$ (**2**)		$[Me_2NC(N^iPr)_2]_3Al_2$ (**3**)		$[Me_2NC(N^iPr)_2]_2AlCl$ (**7**)	
N5−Al−N4	112.7(1)	N2−Al−N9b	119.59(5)	N1−Al−N2	65.72(4)	N4−Al−Cl	120.4(5)
N5−Al−N1	122.7(1)	N9−Al−N9b	120.8(1)	N1−Al−N1b	99.42(4)	N4−Al−N15	118.7(6)
N4−Al−N1	111.7(1)	N2−Al−N9	119.6(5)	N2−Al−N2b	98.86(4)	N15−Al−Cl	121.0(5)
N5−Al−N2	112.8(1)	N4−Al−N4b	157.3(1)	N2−Al−N1b	99.76	N3−Al−N17	165.8(6)
N4−Al−N2	120.9(1)	N9−Al−N4	67.2(7)	N1−Al−N2c	157.4(4)	N4−Al−N3	68.7(6)
N1−Al−N2	70.2(1)	C5−N4−C13	124.88(2)	C9−N1−C1	121.8(1)	N15−Al−N17	68.2(6)
C9−N1−C1	124.9(2)	C5−N4−Al	90.2(1)	C9−N1−Al	91.59(8)	C5−N3−C9	121.5(1)
C9−N1−Al	89.9(2)	C13−N4−Al	140.3(1)	C1−N1−Al	143.2(9)	C5−N3−Al	89.6(1)
C1−N1−Al	136.6(2)	C5−N9−C10	121.2(2)	C9−N2−C4	122.1(1)	C9−N3−Al	137.0(1)
C9−N2−C4	125.0(2)	C5−N9−Al	91.9(1)	C9−N2−Al	91.44(8)	C5−N4−C12	122.4(1)
C9−N2−Al	89.6(2)	C10−N9−Al	139.2(1)	C4−N2−Al	143.2(9)	C5−N4−Al	91.5(1)
C4−N2−Al	131.7(2)	C5−N6−C7	121.1(2)	C9−N3−C7	120.4(1)	C12−N4−Al	139.0(1)
C11−N4−C10	110.2(3)	C5−N6−C8	121.8(2)	C9−N3−C8	121.8(1)	C5−N6−C8	122.4(2)
C11−N4−Al	124.0(2)	C7−N6−C8	116.3(2)	C7−N3−C8	115.5(1)	C5−N6−C7	121.7(2)
C10−N4−Al	124.3(2)	C3−N2−C3b	111.9(2)	Al−N1−C9−N2	0.2(1)	C8−N6−C7	115.3(2)
C13−N5−C12	110.4(3)	C3−N2−Al	124.1(1)	N2−C9−N3−C8	41.0(1)	Al−N3−C4−N5	0.4(2)
C13−N5−Al	123.3(2)	C3−N2−Al	124.1(1)			Al−N15−C16−N17	2.4(2)
C12−N5−Al	124.4(2)	Al−N4−C5−N6	2.69(2)			N3−C5−N6−C7	28.1(2)
Al−N1−C9−N2	2.6(2)	Alb-N4b−C5b−N6b	2.6(2)			N17−C16−N18−C19	30.7(2)
N1−C9−N3−C7	23.5(2)	N4−C5−N6−C7	35.1(2)			Σ angles	
		Σ angles				N6	359
		N6	359.1			N18	358

$[Me_2NC(N^iPr)_2]Ga(NMe_2)_2$ (**4**)		$[Me_2NC(N^iPr)_2]_2GaNMe_2$ (**5**)		$[Me_2NC(N^iPr)_2]_3Ga$ (**6**)	
N4−Ga−N5	112.37(1)	N3−Ga−N10	118.04(1)	N1−Ga−N2	63.86(6)
N4−Ga−N1	110.7(2)	N10−Ga−N17	120.4(1)	N1−Ga−N1b	99.78(5)
N5−Ga−N1	124.7(2)	N3−Ga−N17	121.6(1)	N2−Ga−N2b	99.17(5)
N5−Ga−N2	112.9(2)	N5−Ga−N22	157.2(1)	N1−Ga−N2b	102.0(6)
N4−Ga−N2	122.5(2)	N10−Ga−N5	65.0(1)	N1−Ga−N2c	154.7(6)
N1−Ga−N2	67.6(2)	N17−Ga−N22	64.4(1)	C9−N1−C1	122.4(1)
C9−N1−C1	125.6(4)	C6−N5−C15	123.6	C9−N1−Ga	92.13(9)
C9−N1−Ga	91.2(3)	C6−N5−Ga	123.6(3)	C1−N1−Ga	141.5(1)
C1−N1−Ga	135.8(3)	C15−N5−Ga	139.0(2)	C9−N2−C4	122.5(1)
C9−N2−C4	123.1(4)	C6−N10−C12	122.8(3)	C9−N2−Ga	91.9(1)
C9−N2−Ga	91.0(3)	C6−N10−Ga	94.6(2)	C4−N2−Ga	141.5(1)
C4−N2−Ga	129.9(3)	C12−N10−Ga	135.6(2)	C9−N3−C7	121.0(2)
C11−N4−C10	112.7(4)	C6−N7−C8	121.1(3)	C9−N3−C8	121.8(2)
C11−N4−Ga	122.0(4)	C6−N7−C9	122.6(3)	C7−N3−C8	114.9(2)
C10−N4−Ga	121.3(3)	C8−N7−C9	115.1(3)	Ga−N1−C9−N2	0.4(2)
C13−N5−C12	112.1(4)	C2−N3−C4	114.6(3)	N2−C9−N3−C8	40.3(2)
C13−N5−Ga	120.7(3)	C2−N3−Ga	124.5(3)		
C12−N5−Ga	120.1(3)	C4−N3−Ga	120.8(3)		
Ga−N1−C9−N2	2.6(4)	Ga−N5−C6−N10	1.6(3)		
N1−C9−N3−C7	36.1(4)	Ga−N22−C18−N17	0.9(3)		
		N5−C6−N7−C8	31.6(3)		
		N17−C18−N19−C21	46.4(3)		
		Σ angles			
		N7	358.8		
		N19	358.9		

N centers (C). If this contribution is significant, two structural features should be observed. The NR'_2 center should be planar and sp^2 hybridized, allowing the p-orbital-localized lone pair to overlap with the NCN moiety. In addition, there should be a small torsion angle between the plane NR'_2 group and that defined by the NCN chelate for maximum π bonding.

Scheme 3. Possible Resonance Structures Showing the Planarity of the Exocyclic Nitrogen in the Guanidinate Structure

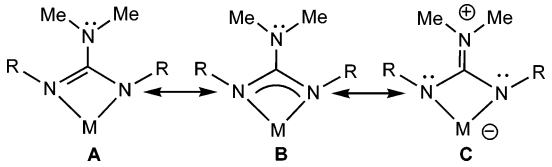

The structural features observed in **1** and **4** support a significant contribution from structure C. As well as a planar N(3) center, the torsion angles defined by M−N1−C9−N2 are 2.6° for both **1** and **4**, showing that the ring nitrogens are both nonplanar. The nonplanar N(1) and N(2) centers are also consistent with structure C and a significant lone pair electron density on these centers leading to the observed pyramidalization. Finally, the torsion angle of N1−C9−N3−C7 is 23.5° in **1** and 36.1° in **4**, along with the N3−C9 bond length, suggests that the exocyclic nitrogen is experiencing some degree of π bonding with the chelate ring in both structures.

The single-crystal X-ray diffraction results for compounds **2**, **5**, and **7** are summarized in Figure 3 and Tables 1 and 2. The structure of **5** is excluded from Figure 3 because it is isostructural with **2**. As it is, compounds **2**, **5**, and **7** share several structural similarities. Only **2** possesses a strict C_2 axis of symmetry, but the slight deviations of **3** and **7** suggest that all three complexes can be treated as having metal centers in pseudotrigonal bipyramidal coordination geometries of approximately C_2 symmetry. All three compounds possess three equatorial groups (e.g., N2, N9, and N9b for **2**; N3, N10, and N17 for **5**; and Cl, N4, and N15 for **7**) that are coplanar with the sum of the angles between these groups equal to 360°. The angle between the pseudoaxial positions shows a similar distortion for the three complexes, which we attribute to the limited bite angle of the guanidinato ligand. In compounds **2** and **5**, this angle is observed to be 157°, with a slightly larger value of 166° for **7**. As expected, the equatorial M−N bonds in **2**, **5**, and **7** were shorter than the axial distances. These differences are larger for **2** (δ = 0.19 Å) and **5** (δ = 0.17 Å) than for **7** (δ = 0.06 Å).

The guanidinate ligands in these compounds exhibit similar bonding parameters as those seen in complexes **1** and **3**, which again suggests a significant contribution of resonance structure C (Scheme 3) to the bonding in these bis(guanidinato) compounds. Specifically, the guanidinate exocyclic N centers are planar and the dihedral angles between these groups and the chelate NCN planes fall in the range of 28.1−46.4° (Table 2). These two features are consistent with the partial π conjugation of these groups. In addition, the nitrogen centers in the guanidinato chelate ring show similar deviations from planarity. For example, in **2**, the sum of angles around N4 and N9 are 355° and 352°, respectively. The analogous angles in **5** have an average value of 352°, and those in **7** have an average value of 351°. There appears to be some correlation of this distortion with steric congestion at the metal center, with the larger deformations observed for **2** and the smallest for **5**.

Single-crystal X-ray diffraction analyses have also been carried out on the hexacoordinate species **3** and **6**. The results of these studies are illustrated in Figure 4 and summarized in Tables 1 and 2. Both structures are symmetrical pseudo-octahedral species possessing only one unique guanidinate ligand, as indicated by the NMR data. The limitations imposed by the bite angle of the guanidinate ligand (65.72° in **3** and 63.86° in **6**) lead to distortions of these structures from ideal octahedral geometries. Thus, the ideal 180° axes are reduced to 157.4° and 154.7° in **3** and **6**, respectively. The M−N bonds are only slightly longer than those observed for **1**−**4**, with values of 2.024 Å in **3** and 2.086 Å and 2.095 Å in **6**. In contrast to the mono- and bis(guanidinato) species, the chelate rings in these complexes are planar, as indicated by the near-zero values of the M−N1−C9−N2 angles (Table 2). The C−NMe_2 groups are planar ($\sum$ angles = 357.7°) in both species. The relatively large angles between the exocyclic nitrogen planes and the NCN planes for these compounds, with values of 40.3° for **3** and 41.0° for **6**, and the longer C9−N3 bond lengths indicate less π overlap between these moieties. These features indicate that B, rather than C (Scheme 3), is the dominant ligand resonance structure for these two species.

Given the potential of species **1**−**6** in vapor-phase thin film syntheses (chemical vapor deposition or atomic layer deposition), it is pertinent to note that the mass spectrometry

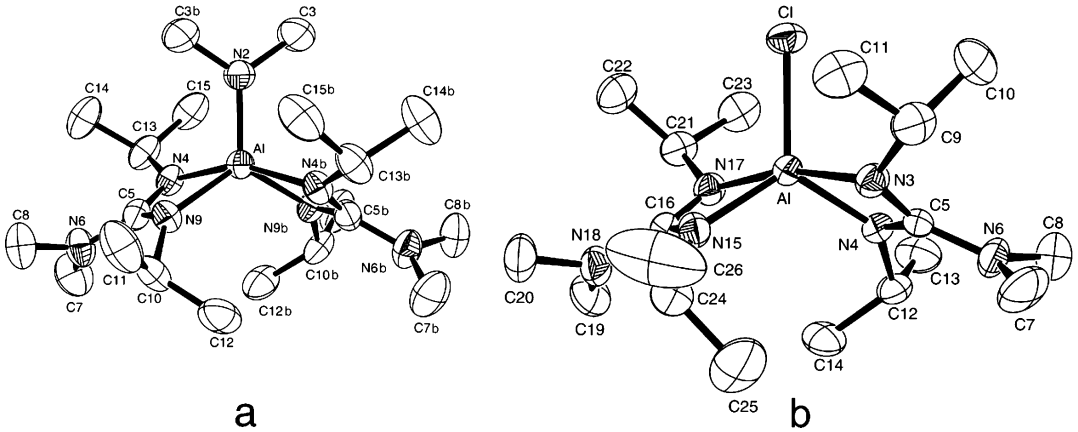

Figure 3. Molecular structure and atom numbering scheme for compounds **2** (a) and **7** (b). Hydrogen atoms have been omitted in every case for clarity, and thermal ellipsoids are shown at 50% probability.

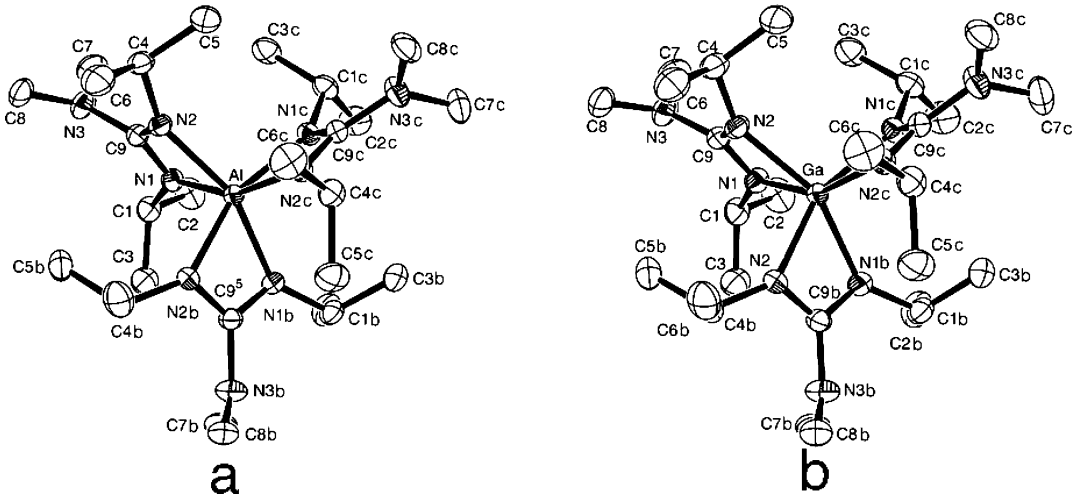

Figure 4. Molecular structure and atom numbering scheme for compounds **3** (a) and **6** (b). Hydrogen atoms have been omitted in every case for clarity, and thermal ellipsoids are shown at 50% probability

data for **1**, **2**, and **4** indicate the presence of a parent ion peak for the mononuclear species and no evidence of dimerization or oligomerization. The highest mass peak observed for compound **3** had an *m*/*e* value of 283, which is consistent with the fragment $[Me_2NC(N^iPr)_2]Ga(NMe_2)^+$ derived by the loss of one dimethylamido group from a monomeric species. All six of these compounds exhibited clean melting points and may offer the potential to be used as liquid precursors.

Conclusions

The insertion of carbodiimides into group 13 metal−amide bonds has been shown to be a facile way to synthesize homoleptic, six-coordinate guanidinato complexes of aluminum and gallium, as well as to make mixed guanidinato−amido compounds for these metals. The compounds are volatile solids and show no thermal decomposition during volatilization, which suggests that they would be valuable precursors for the vapor deposition of group-13-containing thin films. Their synthesis is straightforward, yet there appears to be two mechanisms involved in reaching a final product using stoichiometric control. Initial rapid insertion (several minutes) reactions of carbodiimide into all of the metal−amido bonds leads to the tris(guanidinate) complexes and unreacted starting metal compound. This is then followed by ligand scrambling to produce the stoichiometric product over a time scale of several hours. Subsequent ligand scrambling has been seen in the case of **3** with aluminum trichloride to produce the mixed guanidinatochloro compound **7**. All seven complexes were structurally characterized, and compounds **1**, **2**, **4**, **5**, and **7** were shown to exhibit structural features within the chelate rings and for the noncoordinated N center, which suggests a zwitterionic resonance structure. Compounds **3** and **6** did not exhibit this structural feature. Finally, steric crowding appears to prevent isopropyl rotation in the guanidinate ligand, and a variable-temperature ^{1}H NMR of **6** showed that this steric locking was circumvented at temperatures above room temperature.

(9) Kormos, B. L.; Cramer, C. J. *Inorg. Chem.* **2003**, *42*, 6691 and references therein.

Experimental

General Procedures. All manipulations were performed in a nitrogen-filled drybox. Aluminum chloride, gallium chloride, lithium dimethylamine, 1,3-diisopropyl carbodiimide, anhydrous hexane, and deuterated benzene were purchased from Aldrich Chemical Co. and used as received. The synthesis of $M_2(NMe_2)_6$ (M = Al, Ga) followed literature procedures.[10] The ^{1}H and ^{13}C NMR were collected on a Varian Gemini-200 or a Bruker 400 MHz spectrometer using the residual protons in the deuterated solvent for reference.

$[Me_2NC(N^iPr)_2]Al(NMe_2)_2$ (1). In a 50 mL flask, $Al_2(NMe_2)_6$ (1.00 g, 3.14 mmol) was dissolved in 20 mL of hexane. Diisopropylcarbodiimide (0.79 g, 6.28 mmol) was diluted in about 1 mL of toluene and then added dropwise to the solution, and the reaction mixture was stirred at room temperature overnight. The volatiles were removed in vacuo, leaving a thick liquid with a slightly yellow color. Compound **1** was crystallized from this mixture at −30 °C as a colorless, microcrystalline solid (1.675 g, 94% yield). mp 60 °C. ^{1}H NMR (400 MHz, C_6D_6): δ 3.20 [sept, 2H, C*H*Me$_2$], 3.00 [s, 12H, AlN(C*H*$_3$)$_2$], 2.25 [s, 6H, CN(C*H*$_3$)$_2$], 1.05 [d, 12H, CH(C*H*$_3$)$_2$]. ^{13}C NMR (C_6D_6): δ 169.0 [*C*N$_3$], 45.1 [*C*HMe$_2$], 41.2 [AlN(*C*H$_3$)$_2$], 38.6 [(*C*H$_3$)$_2$N], 24.4 [CH(*C*H$_3$)$_2$]. Mass spectra *m*/*e* (relative abundance): 285 (23.5) M^+. Anal. Calcd for $C_{13}H_{32}AlN_5$: C, 54.71; H, 11.30; N, 24.54. Found: C, 54.41; H, 11.18; N, 24.45.

$[Me_2NC(N^iPr)_2]_2AlNMe_2$ (2). In a 50 mL flask, $Al_2(NMe_2)_6$ (1.16 g, 3.64 mmol) was dissolved in 20 mL of hexane. The dropwise addition of diisopropylcarbodiimide (1.839 g, 14.57 mmol) to this solution resulted in a clear, slightly yellow solution, which was stirred overnight. The volatiles were removed in vacuo, leaving a slightly yellow colored microcrystalline powder (2.675 g, 89% crude yield). Further purification was needed because ^{1}H NMR indicated the presence of a small amount of compound **3**. The solid was dissolved in toluene and left to recrystallize by slow evaporation of the solvent at −30 °C. Compound **2** was collected as clear, colorless crystals (2.52 g, 84% yield). mp 70 °C. ^{1}H NMR (400 MHz, C_6D_6): δ 3.51 [sept, 4H, C*H*Me$_2$], 2.87 [s, 6H, AlN(C*H*$_3$)$_2$], 2.46 [s, 12H, CN(C*H*$_3$)$_2$], 1.35 [br, 12H, CH(C*H*$_3$)$_2$], 1.27 [br, 12H, CH(C*H*$_3$)$_2$]. ^{13}C NMR (400 MHz, C_6D_6): δ 170.22 [N*C*NMe$_2$],

(10) For aluminium, see: Waggoner, K. M.; Olmstead, M. M.; Power, P. P. *Polyhedron* **1990**, *9*, 257. For gallium, see: Nöth, H.; Konrad, P. *Z. Naturforsch.* **1975**, *30b*, 681.

45.68 [N*C*HMe$_2$], 41.81 [AlN(*C*H$_3$)$_2$], 39.33 [CN(*C*H$_3$)$_2$], 24.57 [CH(*C*H$_3$)$_2$]. Mass spectra *m*/*e* (relative abundance): 411 (0.1) M$^+$. Anal. Calcd for $C_{20}H_{46}AlN_7$: C, 58.36; H, 11.26; N, 23.82. Found: C, 58.08; H, 11.02; N, 23.83.

[Me$_2$NC(N^{i}Pr)$_2$]$_3$Al (3). In a 50 mL flask, Al$_2$(NMe$_2$)$_6$ (3.00 g, 9.42 mmol) was dissolved in 25 mL of hexane. Diisopropylcarbodiimide (7.134 g, 56.53 mmol) was diluted in 15 mL of hexane and added dropwise to the solution, resulting in a translucent, slightly yellow solution. The reaction mixture was allowed to stir at room temperature, and a white precipitate formed during this process. Colorless microcrystalline **3** was collected by filtration. The remaining solution was cooled to −30 °C, and further **3** was precipitated and collected by filtration (combined yield: 8.69 g, 86% yield). mp 193 °C. ^{1}H NMR (200 MHz, C$_6$D$_6$): δ 3.67 [sept, 6H, C*H*Me$_2$], 2.66 [s, 18H, CN(C*H*$_3$)$_2$], 1.46 [d, 18H, CH(C*H*$_3$)$_2$], 1.37 [d, 18H, CH(C*H*$_3$)$_2$]. ^{13}C NMR (400 MHz, C$_6$D$_6$): δ 167.9 [N*C*NMe$_2$], 45.8 [N*C*HMe$_2$], 39.9 [CN(*C*H$_3$)$_2$], 26.3 [CH(*C*H$_3$)$_2$], 24.3 [CH(*C*H$_3$)$_2$]. Mass spectra *m*/*e* (relative abundance): 538 (0.1) M$^+$. Anal. Calcd for $C_{27}H_{60}AlN_9$: C, 60.30; H, 11.24; N, 23.44. Found: C, 59.98; H, 11.21; N, 23.14.

[Me$_2$NC(N^{i}Pr)$_2$]Ga(NMe$_2$)$_2$ (4). In a 50 mL flask, Ga$_2$(NMe$_2$)$_6$ (3.00 g, 7.43 mmol) was dissolved in 20 mL of hexane. Diisopropylcarbodiimide (1.875 g, 14.86 mmol) was diluted in about 2 mL of hexane and then added dropwise to the solution. The reaction mixture was allowed to stir at room temperature for 2 days. The volatiles were removed in vacuo, leaving a viscous liquid with a slightly yellow color. Compound **4** was crystallized from hexane at −30 °C as a slightly yellow microcrystalline solid (4.60 g, 94% yield). mp 49 °C. ^{1}H NMR (400 MHz, C$_6$D$_6$): δ 3.26 [sept, 2H, C*H*Me$_2$], 3.06 [s, 12H, GaN(C*H*$_3$)$_2$], 2.28 [s, 6H, CN(C*H*$_3$)$_2$], 1.03 [d, 12H, CH(C*H*$_3$)$_2$]. ^{13}C NMR (C$_6$D$_6$): δ 167.8 [*C*N$_3$], 45.3 [*C*HMe$_2$], 42.6 [GaN(*C*H$_3$)$_2$], 38.9 [(*C*H$_3$)$_2$N], 24.5 [CH(*C*H$_3$)$_2$]. Mass spectra *m*/*e* (relative abundance): 328 (0.1) M$^+$. Anal. Calcd for $C_{13}H_{32}GaN_5$: C, 47.58; H, 9.83; N, 21.34. Found: C, 47.96; H, 10.13; N, 21.05.

[Me$_2$NC(N^{i}Pr)$_2$]$_2$GaNMe$_2$ (5). In a 50 mL flask, Ga$_2$(NMe$_2$)$_6$ (2.00 g, 4.95 mmol) was dissolved in 20 mL of hexane. The dropwise addition of diisopropylcarbodiimide (2.50 g, 19.81 mmol) to this solution resulted in a clear, slightly yellow solution, which was stirred overnight. The volatiles were removed in vacuo leaving a thick liquid with a slightly yellow color. Cooling the solution to −30 °C overnight resulted in the formation of a slightly yellow solid mass (4.425 g, 98% crude yield based on **5**). Further purification was required because ^{1}H NMR indicated the presence of a small amount of compound **6** as an impurity. The solid was dissolved in toluene and left to crystallize by slow evaporation of the solvent at −30 °C. Compound **5** was collected as clear, colorless crystals (1.858 g, 89% yield). mp 45 °C. ^{1}H NMR (400 MHz, C$_6$D$_6$): δ 3.56 [sept, 4H, C*H*Me$_2$], 2.93 [s, 6H, GaN(C*H*$_3$)$_2$], 2.52 [s, 12H, CN(C*H*$_3$)$_2$], 1.34 [d, 24H, CH(C*H*$_3$)$_2$]. ^{13}C NMR (400 MHz, C$_6$D$_6$): δ 167.70 [N*C*NMe$_2$], 46.68 [N*C*HMe$_2$], 41.95 [GaN(*C*H$_3$)$_2$], 40.01 [CN(*C*H$_3$)$_2$], 24.92 [CH(*C*H$_3$)$_2$]. Anal. Calcd for $C_{20}H_{46}GaN_7$: C, 52.87; H, 10.20; N, 21.58. Found: C, 53.10; H, 10.18; N, 21.88.

[Me$_2$NC(N^{i}Pr)$_2$]$_3$Ga (6). In a 50 mL flask, Ga$_2$(NMe$_2$)$_6$ (2.02 g, 5.00 mmol) was dissolved in about 10 mL of hexane. Diisopropylcarbodiimide (4.05 g, 32.09 mmol, slight excess) was added dropwise to the solution, resulting in a translucent, slightly yellow liquid. Clear, white microcrystalline **6** formed overnight and was collected by filtration. The mother liquor was left to recrystallize by slow evaporation of the solvent at room temperature for 2 days. Additional crystals of **6** were collected by filtration (combined yield: 4.49 g, 77% yield). mp 137 °C. ^{1}H NMR (200 MHz, C$_6$D$_6$): δ 3.74 [sept, 6H, C*H*Me$_2$], 2.65 [s, 18H, CN(C*H*$_3$)$_2$], 1.46 [br, 16H, CH(C*H*$_3$)$_2$], 1.39 [br, 16H, CH(C*H*$_3$)$_2$]. ^{13}C NMR (400 MHz, C$_6$D$_6$): δ 166.51 [N*C*NMe$_2$], 46.69 [N*C*HMe$_2$], 40.08 [CN(*C*H$_3$)$_2$], 26.20 [CH(*C*H$_3$)$_2$], 24.66 [CH(*C*H$_3$)$_2$]. Anal. Calcd for $C_{27}H_{60}GaN_9$: C, 55.86; H, 10.42; N, 21.71. Found: C, 55.81; H, 10.22; N, 21.84.

[Me$_2$NC(N^{i}Pr)$_2$]$_2$AlCl (7). In a 50 mL flask, [Me$_2$NC(N^{i}Pr)$_2$]$_3$Al (**6**; 4.00 g, 7.44 mmol) was dissolved in 15 mL of hexane. In a separate 50 mL flask, AlCl$_3$ (0.496 g, 3.72 mmol) was suspended in 5 mL of hexane and then dissolved by adding ether dropwise (approximately 10 mL). The AlCl$_3$ solution was added to the solution of **6**, and the reaction mixture was stirred overnight. The solvent was partially removed in vacuo and cooled to −30 °C. Compound **7** was collected as clear colorless crystals (2.19 g, 49% yield). ^{1}H NMR (400 MHz, C$_6$D$_6$): δ 3.50 [sept, 4H, C*H*Me$_2$], 2.39 [s, 12H, CN(C*H*$_3$)$_2$], 1.40 [d, 24H, CH(C*H*$_3$)$_2$]. ^{13}C NMR (400 MHz, C$_6$D$_6$): δ 170.29 [N*C*NMe$_2$], 45.44 [N*C*HMe$_2$], 38.90 [CN(*C*H$_3$)$_2$], 24.09 [CH(*C*H$_3$)$_2$]. Mass spectra *m*/*e* (relative abundance): 402 (1.8) M$^+$. Anal. Calcd for $C_{18}H_{40}AlClN_6$: C, 53.65; H, 10.00; N, 20.85. Found: C, 53.71; H, 10.36; N, 21.06.

[Me$_2$NC(N^{i}Pr)$_2$]AlCl$_2$ (8). In a 50 mL flask, [Me$_2$NC(N^{i}Pr)$_2$]$_2$AlCl (**7**; 2.16 g, 5.36 mmol) was dissolved in about 20 mL of hexane. In a separate 50 mL flask, AlCl$_3$ (0.848 g, 7.44 mmol) was suspended in about 5 mL of hexane and then dissolved by adding ether dropwise (about 10 mL). The AlCl$_3$ solution was added to the solution of **7** and stirred overnight. After purification, compound **8** was collected as clear colorless crystals (2.18 g, 76% yield). ^{1}H NMR (400 MHz, C$_6$D$_6$): δ 3.06 [sept, 2H, CHMe$_2$], 1.99 [s, 6H, CN(CH$_3$)$_2$], 1.04 [d, 12H, CH(CH$_3$)$_2$]. Mass spectra *m*/*e* (relative abundance): 267 (4.3) M$^+$.

Structural Determinations for Compounds 1−7. Single crystals were mounted on thin glass fibers using viscous oil and then cooled to the data collection temperature. Crystal data and details of the measurements are included in the Supporting Information. Data were collected on a Bruker AXS SMART 1k CCD diffractometer using 0.3° ω scans at 0, 90, and 180° in ϕ. Unit-cell parameters were determined from 60 data frames collected at different sections of the Ewald sphere. Semiempirical absorption corrections based on equivalent reflections were applied. The structures were solved by direct methods, completed with difference Fourier syntheses, and refined with full-matrix least-squares procedures based on F^2. All non-hydrogen atoms were refined with anisotropic displacement parameters. All hydrogen atoms were treated as idealized contributions. All scattering factors and anomalous dispersion factors are contained in the SHELXTL 5.1 program library.

Acknowledgment. The authors thank Patrick Bazinet for help with the structures of **1** and **4** and Xiang Ouyang for help with the structures of **2** and **5**. D.S.R. thanks NSERC for financial support. S.T.B. thanks Carleton University for financial support.

Supporting Information Available: Crystallographic information files (CIF) for compounds **1**−**7** and structures for compounds **4** and **5**. This material is available free of charge via the Internet at http://pubs.acs.org.

IC048433G